High-speed dynamics, damping, and relaxation times in submicrometer spin-valve devices

Stephen E. Russek[a] and Shehzaad Kaka
Electromagnetic Technology Division, National Institute of Standards and Technology, Boulder, Colorado 80303

Michael J. Donahue
Mathematical and Computational Sciences Division, National Institute of Standards and Technology, Gaithersburg, Maryland 20899

The dynamical response of spin-valve devices with linewidths of 0.8 μm has been measured after excitation with 160 ps magnetic impulses. The devices show resonant frequencies of 2–4 GHz which determine the upper limit of their operation frequency. The dynamical response can be fit with Landau–Lifshitz models to extract an effective uniform-mode damping constant, α_{um}. The measured values of α_{um} were between 0.04 and 0.01 depending on the magnitude of the longitudinal bias field. The appropriate damping coefficient for use in micromagnetic modeling, α_{mm}, was extracted from the dynamical response with large longitudinal bias field. This value was used to model the switching of a 0.1 μm$\times$1.0 μm magnetoresistive random access memory cell. The micromagnetic model included shape disorder that is expected to be found in real devices. The simulations showed that, while the magnetization reverses rapidly ($<$0.5 ns), it took several nanoseconds for the energy to be removed from the magnetic system. The switching energy was stored in short wavelength magnetic fluctuations that could dramatically affect the re-reversal process 1–2 ns after the first reversal. [S0021-8979(00)70908-X]

I. INTRODUCTION AND DEVICE STRUCTURE

High speed operation of giant magnetoresistance recording heads and magnetoresistive random access memory circuits in the gigahertz frequency range will require a detailed understanding of the dynamics of submicrometer magnetic devices.[1,2] The dynamics of small magnetic devices is expected to be different from that measured in single-layer magnetic films[3–6] due to the large magnetostatic fields, shape disorder, interface disorder, interlayer coupling, and different magnetic excitation spectra. In this article we present data that clearly show the dynamical behavior of small spin-valve devices. The resonant frequencies of the devices, which determine their maximum operation frequency, were 2–4 GHz, depending on the longitudinal bias field. We extract damping constants and determine the effect of the damping constant on micromagnetic calculations of switching.

The GMR devices used for this work were spin valves with a synthetic antiferromagnet pinned layer. The films were sputter deposited on thermal SiO_2 layers on high resistivity Si wafers with a layer structure of: Ta 5.0 nm–$Ni_{0.8}Fe_{0.2}$ 5.0 nm–Co 1.0 nm–Cu 3.0 nm–Co 2.0 nm–Ru 0.6 nm–Co 1.5 nm–FeMn 10 nm–Ta 5.0 nm. This device structure was chosen because the pinning field is very large ($>$0.2 T) and the interactions between the free and pinned layers are minimized due to the low net moment of the pinned layer. The magnetization dynamics will be predominantly confined to the free layer and the device can be modeled as a single dynamic layer.

The magnetoresistance, ΔR, is proportional to the projection of the free layer magnetization, $\mathbf{M}_f$, onto the pinned layer magnetization, $\mathbf{M}_p$. By varying the pinned layer direction the magnetoresistance provides a high bandwidth probe of any component of the average free-layer magnetization of the device between the contact electrodes.

II. HIGH-SPEED ROTATION

High-speed rotation of the magnetization was measured by incorporating spin-valve devices into a high-speed measurement structure.[7] A current pulse is sent down a 50 Ω impedance microstrip write line to create a magnetic field pulse. The device, which lies underneath the write line, is connected to a 50 Ω impedance microstrip sense line. A constant 1.0–2.0 mA bias current is put through the sense line and the device. The high-frequency voltage signal, which is proportional to ΔR, is taken off the sense line through a bias tee.

Figure 1 shows positive and negative magnetic field pulses, with pulse widths of 160 ps, and the corresponding MR response for a 0.8 μm$\times$4.8 μm device. The magnetic field and pinned direction are along the transverse (hard) axis of the device and the MR response is proportional to the average transverse magnetization. For the pulsed field values shown in Fig. 1, $\mathbf{M}_f$ is rotated close to 90°. Two response regimes can be seen. In the first (from 1.4 to 1.9 ns), the device magnetization rapidly rotates to 90° under the influence of the applied field, remains there for approximately 300 ps, and then rapidly rotates back along the device axis, driven predominantly by shape anisotropy. In the second (from 2 to 4 ns), the magnetization undergoes a damped

[a]Electronic mail: russek@boulder.nist.gov

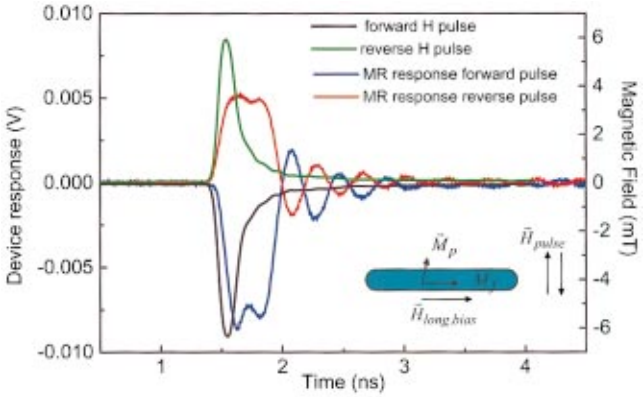

FIG. 1. (Color) Positive and negative applied magnetic fields pulses, with 160 ps pulse width, and the corresponding MR response of a 0.8 μm×4.8 μm spin-valve device with no longitudinal bias. The magnetic field amplitude is approximated as follows: $H_p = V_{av}/2RW$, where V_{av} is the average of the incident and transmitted voltage pulse, R is the impedance of the line, and W is the width of the write line.

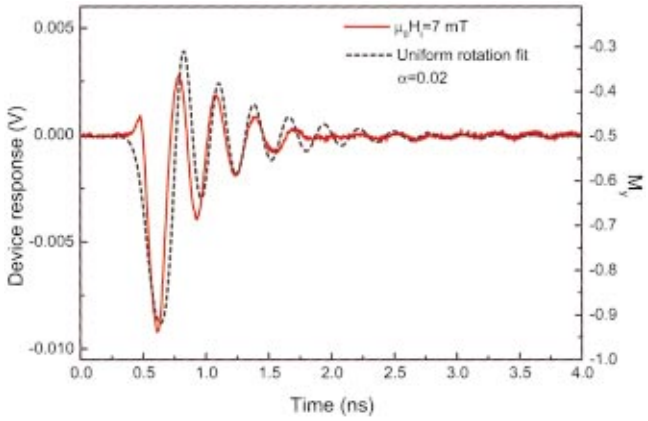

FIG. 3. (Color) The MR response and uniform-rotation-model fit, with $\alpha_{um}=0.02$, for a 0.8 μm×4.8 μm device with 7 mT longitudinal bias.

oscillation until it reaches its quiescent state along the easy axis. Micromagnetic simulations[8] indicate that the complicated double-peak structure seen during the first phase is due to the magnetization at the center of the device rotating beyond 90° after the applied field is removed, with the edge magnetization rotating only slightly. The response to the positive and negative field pulses are asymmetric, with the negative response being somewhat larger than the positive response. This is due to the pin direction deviating slightly (15°) from the transverse direction and to the coupling between the free layer and the pinned layer which causes the quiescent magnetization to point slightly toward the pinned direction. The damped oscillations or ''ringing'' can be seen to persist for 2 ns after the field pulse, indicating that the system is underdamped.

Figure 2 shows the response to a negative field impulse as a function of longitudinal bias field. As the longitudinal bias field is increased, the response decreases and the oscillation frequency increases since the bias field adds to the easy-axis anisotropy field, increasing the restoring force. The inset shows that the resonant frequency increases from 2.4 to 4.2 GHz as the bias field is increased from 0 to 14.0 mT. Also shown are the device responses, with no longitudinal bias, for two different pulsed field values, one just at the saturation value and one 5 dB larger. It is clear that the device is close to saturation since the MR response does not increase substantially. The more pronounced double-peak structure for the larger field pulse is due to the increased nonuniformity of the magnetization; the micromagnetic simulations indicate that the center of the device can rotate well beyond 90°.

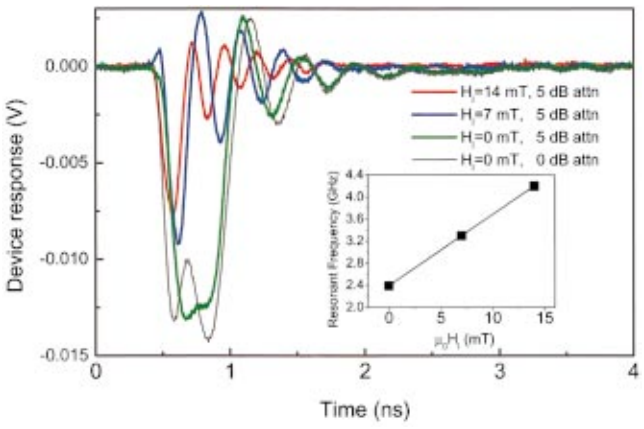

FIG. 2. (Color) Response of 0.8 μm×4.8 μm spin valve in response to a 160 ps negative field pulse for different values of longitudinal field bias and pulse amplitude. The inset shows the oscillation frequency as a function of longitudinal bias.

Figure 3 shows a fit to the rotation data, for 7 mT longitudinal bias field, using a single domain Landau–Lifshitz model. Although the data and micromagnetic simulations show clearly that the uniform rotation model is not correct, especially when the magnetization is rotated through large angles, the fits give an effective uniform-mode damping constant α_{um}, which measures approximately how fast the average magnetization is damped. α_{um} is 0.02 for the data shown in Fig. 3 and α_{um} shows a systematic decrease, as the longitudinal bias is increased from 0 to 14.0 mT.[9]

The energy transferred by the magnetic field pulse is initially imparted to the long wavelength magnetic structure and the associated anisotropy, exchange, and magnetostatic energies.[10] The energy is then transferred to short wavelength magnetic structure, phonons, and other electronic degrees of freedom. For micromagnetic simulations, the energy transfer to short wavelength magnetic excitations is contained in the model, provided that the correct defect structure is included. To find the appropriate damping constant for micromagnetic simulations we need to separate the energy flow to the short wavelength magnetic structure from the other loss mechanisms. If we assume that only the energy transfer from the long to short wavelength magnetic structure is dependent on rotation angle, then the upper limit of the damping coefficient required for micromagnetic calculations, α_{mm} can be taken as the smallest value of α_{um} measured at large longitudinal bias. For the present device structure, $\alpha_{mm} < 0.02$.

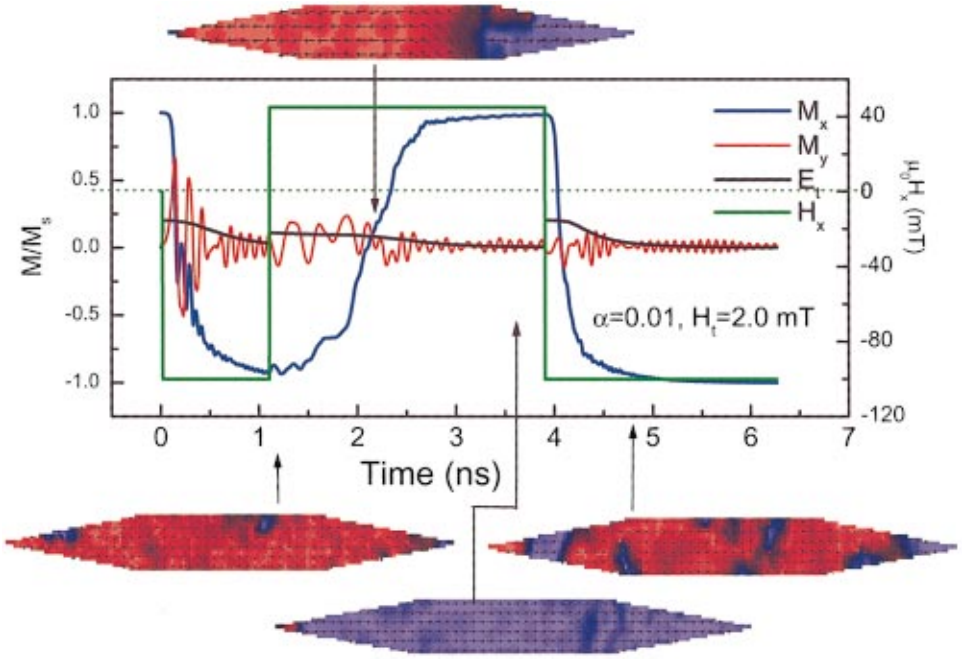

FIG. 4. (Color) Micromagnetic simulation of switching in a 0.1 μm×1.0 μm tapered element for a series of field reversals. Shown are the longitudinal magnetization M_x, the transverse magnetization M_y, the total energy E_t, and the longitudinal applied field H_x as a function of time. At $t=0$, −100 mT longitudinal field is applied; at $t=1.2$ ns, 40 mT longitudinal field is applied; and at 3.9 ns, −100 mT longitudinal field is applied. The device edge roughness and left–right asymmetry provide enough disorder to break up the long wavelength magnetic structure rapidly.

III. SIMULATION OF HIGH-SPEED SWITCHING

The use of the correct damping parameter and the inclusion of disorder in micromagnetic simulations of magnetic devices are essential in determining the high-speed operation characteristics of small magnetic devices. This is illustrated in Fig. 4, which shows a micromagnetic simulation of the reversal of a 0.1 μm×1.0 μm tapered cell using a value of $\alpha_{\mathrm{mm}}=0.01$ and a transverse bias field of 20 mT. The bit has irregular edges plus a slight left-to-right asymmetry to model some of the effects of shape disorder. The magnetization starts pointed to the right (positive); at $t=0$ we apply a −100 mT pulse toward the left. The longitudinal component of the magnetization, M_x, shows an initial rapid reversal; however, a long tail in M_x can be observed. The simulations show that while the magnetization predominantly switches, large magnetic fluctuations are seen that reduce the magnitude of the average magnetization below the saturation magnetization. These fluctuations, which are analogous to high temperature thermal fluctuations, decay with a time constant proportional to $1/\alpha_{\mathrm{mm}}$. For this value of α_{mm} we see that the fluctuation can persist for 1–2 ns. Figure 4 shows that if we apply a field pulse of 40 mT at $t=1.2$ ns before the fluctuations have died out, the device will switch. This field is well below the quiescent switching field of 62 mT. This example demonstrates that, for reproducible switching, one must wait for the energy to be transferred out of the magnetic system. Hence, knowing the value for α_{mm} is essential in determining and modeling the high-speed performance of magnetic devices.

ACKNOWLEDGMENTS

We acknowledge the support of the DARPA Spintronics program and the NIST Advanced Technology Program and useful discussions with Tom Silva and Pavel Kabos.

[1] B. A. Everitt, A. V. Pohm, R. S. Beech, A. Fink, and J. M. Daughton, IEEE Trans. Magn. **34**, 1060 (1998).
[2] R. H. Koch *et al.*, Phys. Rev. Lett. **81**, 4512 (1998).
[3] C. D. Olson and A. V. Pohm, J. Appl. Phys. **29**, 274 (1958).
[4] W. Dietrich, W. E. Proebster, and P. Wolf, IBM J. Res. Dev. **4**, 189 (1960).
[5] W. K. Hiebert, A. Stankiewicz, and M. R. Freeman, Phys. Rev. Lett. **79**, 1134 (1997).
[6] T. J. Silva, C. S. Lee, T. M. Crawford, and C. T. Rogers, J. Appl. Phys. **85**, 7849 (1999).
[7] S. E. Russek, J. O. Oti, S. Kaka, and E. Y. Chen, J. Appl. Phys. **85**, 4773 (1999).
[8] Micromagnetic simulations were done using the NIST OOMMF modeling package (http://math.nist.gov/oommf/). The 0.8 and 0.1 μm devices were simulated using a cell size of 10 and 3 nm, respectively. The shape of the 0.8 μm devices was taken from atomic force microscopy images.
[9] The variation of the damping constant is similar to that seen in dynamical measurements of single-layer films (see, for instance, Ref. 6).
[10] H. B. Callen, J. Phys. Chem. Solids **4**, 256 (1958).